

Tailoring graphene with metals on top

B. Uchoa,¹ C.-Y. Lin,² and A. H. Castro Neto¹

¹Physics Department, Boston University, 590 Commonwealth Avenue, Boston, Massachusetts 02215, USA

²IBM Almaden Research Center, San Jose, California 95120, USA

(Received 13 September 2007; published 17 January 2008)

We study the effects of metallic doping on the electronic properties of graphene using density functional theory in the local density approximation in the presence of a local charging energy. The electronic properties are sensitive to whether graphene is doped with alkali or transition metals. We estimate the charge transfer from a single layer of potassium on top of graphene in terms of the local charging energy of the graphene sheet. The coating of graphene with a *nonmagnetic* layer of palladium, on the other hand, can lead to a magnetic instability in coated graphene due to the hybridization between the transition metal and the carbon orbitals.

DOI: [10.1103/PhysRevB.77.035420](https://doi.org/10.1103/PhysRevB.77.035420)

PACS number(s): 73.20.At, 71.15.Mb

I. INTRODUCTION

Graphene, a two dimensional allotrope of carbon on a honeycomb lattice, is characterized by elementary electronic excitations described in terms of Dirac fermions,¹ a solid state realization of a relativistic system.² The observation of theoretically predicted^{3,4} anomalous plateaus in the quantum Hall effect^{5,6} and of a universal minimum of conductivity⁵ attracted a lot of interest. In the absence of doping, graphene behaves as an unusual metal with low density of states.⁷ Because the linear band spectrum is a robust feature of the honeycomb lattice, the excitations in graphene are particles with zero effective mass, which propagate coherently very large distances disregarding the amount of impurities, allowing graphene to sustain supercurrents.⁸ By applying a bias voltage, the carrier density of graphene can be controlled by electric field effect allowing for many practical applications ranging from the production of electronic lenses⁹ to the fabrication of semiconductors with a tunable gap in bilayers.¹⁰

One of the roads still unexplored in the materials science of graphene is the tailoring of its electronic properties by chemically adsorption of metallic atoms. The electronic properties that result from adsorption depend strongly on the ionic and/or covalent character of the bonds formed between carbon and the metal. Alkaline metals are good electron donors because of the strong ionic character of their bonding, increasing dramatically the number of charge carriers in graphene.¹¹ At the same time, the metallic bands can be strongly affected by the presence of the graphene lattice, as observed in some graphite intercalated compounds (GICs).¹² On theoretical grounds, both effects can produce superconductivity in coated graphene.¹³ Transition metals by their turn tend to make strong covalent bonds. Because of the strong electron-electron interactions in these materials, they are more susceptible to induce magnetic instabilities. The tuning of magnetism in coated graphene can open other routes to spintronics through new spin-valve devices. Similar effects have been studied in the context of carbon nanotubes.¹⁴

We study the effect of metallic coating of graphene using two different metal atoms: potassium (K) and palladium (Pd). Among alkaline metals, K atoms have a particularly good matching with the graphene lattice and their adsorption

on graphite surfaces has been a topic of extensive research.¹⁵ We address the problem of charge transfer between K and graphene and discuss the nature of the K conduction band in coated graphene. Although there are many transition atoms that interact strongly with carbon,¹⁶ Pd has very polarizable bands and, hence, is a natural candidate for the generation of magnetism in coated graphene.

II. NUMERICAL CALCULATION

We investigate the electronic properties of coated graphene from a band structure calculation based in density functional theory (DFT) in local density approximation (LDA). In order to study a single layer of graphene, we repeat graphene layers periodically with 33.6 Å of vacuum separation. The electronic structure is calculated using the all-electron full-potential linearized augmented plane wave method¹⁷ with corrections to the exchange-correlation potential calculated in the generalized gradient approximation (GGA).¹⁸ To further take into account the local interactions, we go beyond GGA assigning a phenomenological parameter U (LDA+ U),^{19,20} which corresponds to the effective local potential between two electrons in the same localized orbital.

A. K coated graphene

In K coated graphene, K atoms sit on top of the hexagons around 2.7 Å away from the graphene plane.²¹ Since K is much larger than carbon, the maximum coverage is achieved at one K atom per eight carbons, KC_8 , which corresponds to one monolayer. In this concentration, we relax the K-graphene distance to 2.68 Å within GGA after the minimization of the interatomic forces is done. Since the C-C bonds are much stronger than the bonds of C with the metal, the effect of the relaxation of the graphene lattice due to the coating is very small.²² We use the lattice parameter of pure graphene, $a=1.42$ Å, in the calculations.

When K is deposited on top of graphene, part of the electrons in the 4s band are transferred to the π^* band of C to compensate for the difference in electronegativities. In this process, the π bands suffer a rigid shift, generating a pocket of electrons with a finite density of charge carriers in the graphene plane. At the same time, there is a significant re-

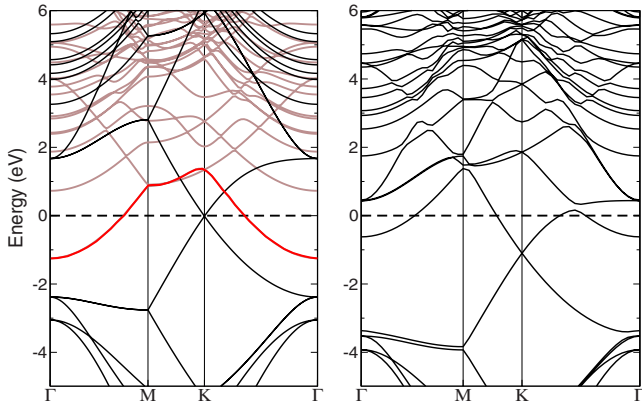


FIG. 1. (Color online) On the left: superposition of the bands for one monolayer of K (red and brown lines) and pure graphene (black lines) in the unit cell of KC_8 . On the right: band plot of KC_8 in GGA ($U=0$).

distribution of charges within the K states, which accompanies the formation of K-C bonds.^{22,23} In the plot in Fig. 1 (left), we show the bands of graphene in the expanded unit cell of KC_8 superimposed with the bands of a freestanding K monolayer. The $4s$ band of K shown in red forms a nearly circular Fermi surface around the center of the Brillouin zone (BZ) at the Γ point, while the π bands of pure graphene cross the Fermi level at the corners of the BZ (K point). After a careful comparison between the high energy bands of KC_8 with the K and graphene bands in separate, we are able to find a nearly one-to-one correspondence in the energy range of 0–6 eV between the empty bands of KC_8 , shown in Fig. 1 (right), and the empty bands of the free K monolayer. However, we find no trace of the graphene nearly free electron (NFE) bands in KC_8 , which in pure graphene start from ~ 3 eV above the Fermi level, as shown in Fig. 1.²⁴ This suggests that the interstitial NFE bands drop to the Fermi level and hybridize with the $4s$ band of K in a similar way to previous band structure analysis on GIC¹² and carbon nanotubes.²⁵ The strong downshift of these high energy bands is an electrostatic response of the graphene NFE bands to the potential induced by the background of positive charge of the K ions.²⁶ This picture indicates that the charge of this system is distributed in the graphene layer and also in the interstitial space of the KC_8 bilayer.

The amount of charge transfer to graphene in KC_8 is still an open question in the literature and has been studied for many years in K deposited graphite surfaces.¹⁵ Previous LDA calculations with specific assumptions on the pseudopotentials have predicted a charge transfer of $\sim 0.17e$ per K (Refs. 21 and 22) on KC_8 and $\sim 0.1e$ per K for one monolayer of K on top of a stack of graphite layers.^{27,28} On the other hand, a recent all-electron GGA cluster method calculation on KC_8 has predicted a substantially larger charge transfer of $0.46e$ per K.²⁹ We remark, however, that because C orbitals are poorly screened by K, the local Hubbard potential in the carbon p_z orbitals is an important input which modifies the difference of electronegativities between graphene and the metal. Indeed, we observe within the LDA+ U framework that the total amount of charge transfer

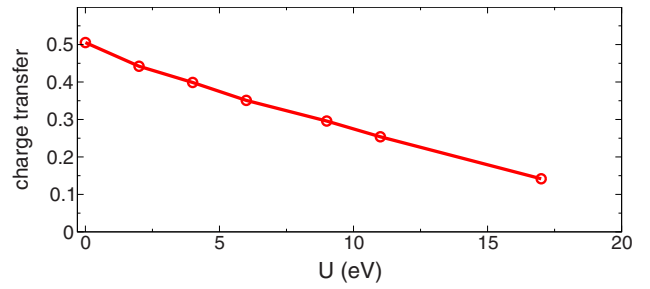


FIG. 2. (Color online) Charge transfer δQ from K to graphene in KC_8 (in electrons per K) as a function of the effective Hubbard U in the C p_z orbitals. The charge transfer for $U=0$ has been calculated in GGA for comparison with Ref. 29.

is very sensitive to U . To estimate the charge transfer, we extract the energy shift of the K $4s$ band (red curve in Fig. 1) when the K layer is deposited on top of graphene. For $U=0$, our DFT calculation predicts a charge transfer of $\delta Q = 0.51e$ per K. As U increases, the charge transfer is linearly suppressed and eventually extrapolates to zero for $U \sim 25$ eV (see Fig. 2). The hopping energy of the electrons in graphene is $t \sim 3$ eV. As in fullerenes,³⁰ if a Hubbard $U \sim 3t$ can be taken as a reasonable estimate for the order of magnitude of U in graphene, then the LDA+ U calculation may lower considerably the amount of charge transfer predicted by a pure GGA calculation.²⁹ On the other hand, since the LDA+ U method does not take polarization effects into account, the local charging energy U can be additionally screened by the pocket of electrons in graphene. Our effective U is a screened local charging energy in the graphene layer.

The electronic density transferred to the graphene layer is $\delta Q/A_K$, where $A_K = 6\sqrt{3}a^2$ is the area of the K unit cell on top of graphene. For a small charge transfer δQ , the shift in the chemical potential of the π bands is

$$\delta\mu = (v_F/a)\sqrt{\pi/(6\sqrt{3})}\delta Q \sim 2.3\sqrt{\delta Q} \text{ (eV)}, \quad (1)$$

where $v_F = 6 \text{ eV \AA}$ is the π^* -band velocity around the K point. Hence, we see that a very small charge transfer of $\delta Q \sim 0.01e$ per K is already enough to exceed the maximum chemical shift achievable by the application of a bias voltage in graphene [≈ 0.2 eV (Ref. 1)]. For a charge transfer larger than $\sim 0.2e$ per K, the shift of the π bands is above 1 eV and reaches $\delta\mu \sim 1.2$ eV for $U=0$, when the charge transfer is maximum (see Fig. 1). A π -band shift of the same order has been very recently measured with angle resolved spectroscopy for K coated graphene (KC_8) on a SiC substrate.³¹ In this experiment, the charge transferred from the substrate shifts the π bands of pure graphene in 0.45 eV, which corresponds to $\sim 0.04e$ per unit cell of KC_8 . The total π -band shift was estimated in ~ 1.2 eV, indicating that each K atom transfers the order of $0.5e$ to graphene. This result contrasts with a recent photoemission experiment for a K monolayer adsorbed on the surface of graphite, which estimated the charge transfer in $\sim 0.1e$ per K.³² According to our DFT results, these experiments suggest that the local charging en-

ergy of graphene is strongly screened by the presence of the SiC substrate (see Fig. 2).

In K intercalated graphite, previous DFT pseudopotential calculations have reported charge transfers larger than $0.7e$ per K.^{33,34} These results may indicate that the character of the K/C bonding is modified by intercalation.³⁴ A more conclusive comparison between GIC with the present results, however, requires a closer examination of the intercalated case through a similar DFT method.

The size control of the charge pockets in graphene can be achieved by dilution of the K coverage. For dilution less than 0.9 of a monolayer, however, K does not form a uniform metallic lattice due to clustering, leading to insulating behavior.¹⁵

B. Pd coating case

Because of the low coordination number, the d orbitals of transition metals can be very localized in systems of low dimensionality. Among $4d$ transition metals, bulk paramagnetic elements such as Ru, Rh, and Pd exhibit magnetism on surfaces and in nanosystems.^{35–37} In particular, Pd atoms are not intrinsically magnetic because of the closed shell configuration of the $4d$ orbitals ($4d^{10}5s^0$). In bulk, the s and d bands of Pd hybridize ($4d^{10-\epsilon}5s^\epsilon$), and Pd exhibits strong Pauli paramagnetism with a high magnetic susceptibility. Due to the high density of states near the Fermi surface, bulk fcc Pd is close to a ferromagnetic instability. Expanding the fcc lattice in 5%, the Stoner criterion is satisfied and Pd becomes an itinerant ferromagnet due to the enhancement of the s - d band hybridization.³⁸

On top of graphite, Pd atoms do not form a uniform metallic coating but large clusters.³⁹ It is not clear to what extent Pd atoms can grow laterally to form islands as Ru (Ref. 35) and Rh (Ref. 40) or if they agglomerate to form clusters of a few layers thick. If we assume that the Pd atoms inside the islands form a low temperature commensurate structure with the graphene lattice with the same periodicity as in Rh adsorbed on the surface of graphite,⁴⁰ the Pd atoms sit at the center of the hexagons of graphene separated by a distance of $\sqrt{3}a \sim 2.46 \text{ \AA}$ from the next Pd neighbor. In this case, the Pd-graphene equilibrium distance is 3.35 \AA , after we minimize the interatomic forces between the Pd and graphene layers. This configuration represents a lateral compression of $\sim 7\%$ with respect to the bond length of Pd in a square lattice,⁴¹ and a very small magnetization is expected as a result of the weak hybridization of the bands.⁴²

Nevertheless, the splitting of the bands due to the hybridization of Pd and graphene orbitals at finite U can produce a strong enhancement of the density of states at the Fermi surface. We show that the Pd bands in coated graphene can strongly polarize through a Stoner transition. We focus in the Pd coating to illustrate the effect of the metal-carbon hybridization in the production of itinerant ferromagnetism. Since the orbitals in the transition metal monolayer are more localized than in graphene, we assign in first approximation a single effective parameter U to the metallic bands in our LDA+ U calculation.

In Fig. 3(b), we show the spectrum of a freestanding monolayer of Pd in the unit cell of graphene. The bands in

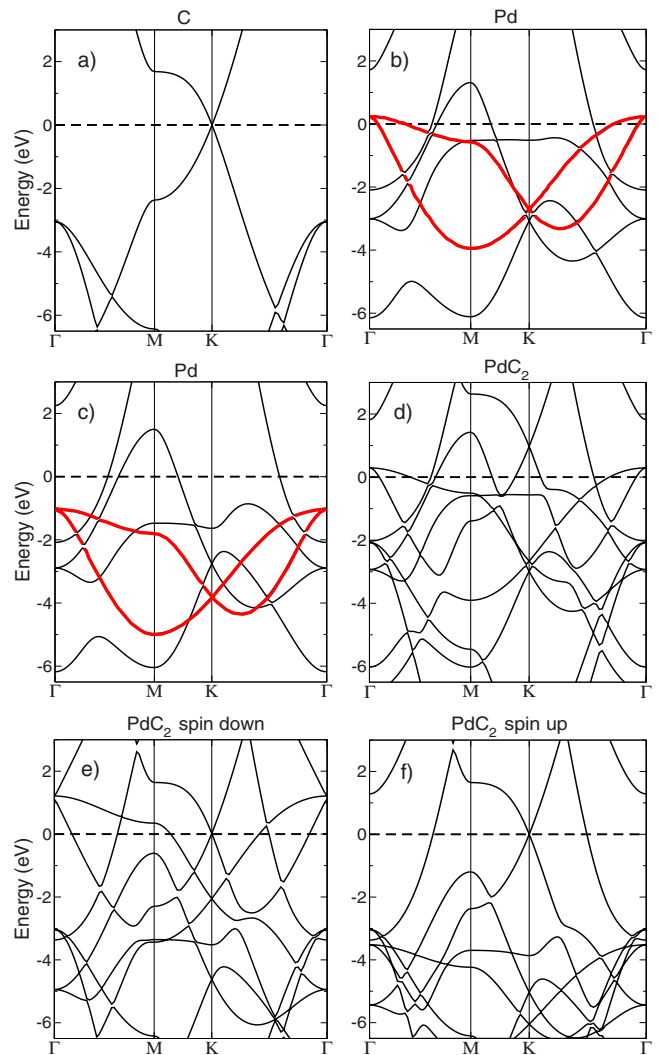


FIG. 3. (Color online) Band plots for (a) graphene, (b) a free-standing monolayer of Pd for $U=0$, and (c) free Pd monolayer for $U=11 \text{ eV}$. In plots (d), (e), and (f), we display the bands of PdC_2 for (d) $U=0$, (e) $U=11 \text{ eV}$ in Pd for spin down, and (f) $U=11 \text{ eV}$ in Pd for spin up.

red can be associated with the Γ point (the center of the BZ) to the two degenerated bands $4d_{xz}$ and $4d_{yz}$ of the free Pd atom. The two bands that cross the Γ point at $\sim -3 \text{ eV}$ can be associated near Γ to the degenerated bands $4d_{xy}$ and $4d_{x^2-y^2}$ of free Pd, while the $5s$ band crosses the Γ point at $\sim -2 \text{ eV}$. Finally, the high energy band which crosses the Γ point at $\sim 6 \text{ eV}$ below the Fermi level corresponds to the $4d_{z^2}$ orbital of free Pd around the center of the BZ.

When we turn on the local potential to $U=11 \text{ eV}$ in the free Pd monolayer [see Fig. 3(c)], we clearly see that the bands in red suffer a rigid downshift of $\sim 1 \text{ eV}$, indicating the presence of localized states in these bands. The band which is nearly flat between points K and M in Fig. 3(b) shifts in $\sim 1 \text{ eV}$ around the border of the BZ (points K and M), where the effects of the lattice symmetry are stronger, and remains unaltered at the center of the BZ, where the $d_{x^2-y^2}$, and d_{xy} orbital symmetries dominate, suggesting that the states around Γ in this band are more delocalized along

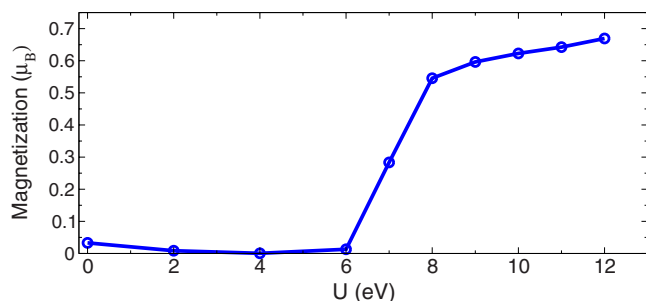


FIG. 4. (Color online) Magnetization of Pd coated graphene, PdC₂ (in Bohr magneton) vs local potential U in the Pd orbitals.

the plane of the Pd monolayer. The other two $4d$ bands and the $5s$ band are almost insensitive to the local potential and are delocalized bands. We do not see any trace of magnetization in the freestanding Pd monolayer for U in the range of 0–12 eV.

In the sequence of plots, in Figs. 3(d)–3(f), we set the Pd monolayer on top of graphene for $U=0$ and then we set U to be finite. Because graphene is more electronegative than Pd, the π band is shifted up in ~ 1 eV for $U=0$. In this case, the d orbitals of Pd strongly hybridize with the graphene p_z orbitals, but the Stoner condition is not satisfied and the system does not magnetize. For $U=11$ eV, however, the π bands nearly recover charge neutrality and the redistribution of charge among the hybridized d orbitals due to the local charging energy enhances dramatically the density of states in the localized bands of Pd at the Fermi surface. In this situation, the Pd bands strongly polarize, as displayed in Figs. 3(e) and 3(f), and we observe a total magnetization of $0.64\mu_B$ in the Pd unit cell (see Fig. 4), indicating a ferromagnetic instability. The strength of the magnetization is very sensitive to the specific value of the assigned local potential for $U \gtrsim 6$ eV, where the Stoner condition is satisfied and the system has a ferromagnetic phase transition, as shown in Fig. 4.

III. SUMMARY AND CONCLUSION

We have explored the electronic properties of graphene coated with alkaline and transition metals from a band struc-

ture calculation in LDA+ U . We propose that graphene can be tailored either by the control of the number of charge carriers, which can be tuned by coating graphene with a controlled coverage of alkaline metals, such as K, or by inducing a ferromagnetic instability in graphene through the coating with a transition metal.

We addressed the problem of the charge transfer between one monolayer of K and graphene, emphasizing the role of the local charging energy in the graphene layer. Our DFT results in coated graphene suggest that the metallic band of K hybridizes with the carbon NFE band in a similar way as previously reported in GIC and carbon nanotubes. We emphasize that the problem of coating is conceptually different from the adsorption of isolated alkaline adatoms in graphene, where the metallic orbitals strongly localize around the impurities. In particular, the estimation of the charge transfer from each K impurity in the dilute phase depends on specific definitions of the atomic charge.⁴³ In graphene coated with a uniform monolayer of K, the K s electrons delocalize and the charge transfer can be accurately estimated by the energy shift of the bands at the Fermi level, as shown in Fig. 1.

The amount of charge transferred from K within the LDA+ U framework is sensitive to the effective local charging energy assigned to the carbon orbitals. For $U=0$, we find a maximum charge transfer of $0.51e$ per K, which is linearly suppressed with the increase of the effective charging energy U . A comparison of our DFT calculation with recent spectroscopy and photoemission experiments suggests that different substrates can give rise to very different values of U in graphene.

For $4d$ transition metals such as Pd, we showed that the hybridization of the graphene p_z orbital with the localized d orbitals at finite U can produce strong itinerant magnetism in coated graphene. The onset of ferromagnetism in Pd coated graphene is identified through a Stoner transition for $U \gtrsim 6$ eV, where the local bands of Pd polarize.

ACKNOWLEDGMENTS

We thank S. Fagan for illuminating discussions. B.U. acknowledges CNPq, Brazil, for the support under Grant No. 201007/2005-3. A.H.C.N. was supported through NSF under Grant No. DMR-0343790.

¹K. S. Novoselov, A. K. Geim, S. V. Morozov, D. Jiang, Y. Zhang, S. V. Dubonos, I. V. Grigorieva, and A. A. Firsov, *Science* **306**, 666 (2004).
²A. H. Castro Neto, F. Guinea, and N. M. Peres, *Phys. World* **19** (11), 33 (2006).
³N. M. R. Peres, F. Guinea, and A. H. Castro Neto, *Phys. Rev. B* **73**, 125411 (2006).
⁴V. P. Gusynin and S. G. Sharapov, *Phys. Rev. Lett.* **95**, 146801 (2005).
⁵K. S. Novoselov, A. K. Geim, S. V. Morozov, D. Jiang, M. I. Katsnelson, I. V. Grigorieva, S. V. Dubonos, and A. A. Firsov, *Nature (London)* **438**, 197 (2005).

⁶Y. Zhang, Y.-W. Tan, H. L. Stormer, and P. Kim, *Nature (London)* **438**, 201 (2005).
⁷A. K. Geim and K. S. Novoselov, *Nat. Mater.* **6**, 183 (2007).
⁸H. B. Heershe, P. Jarillo-Herrero, J. B. Oostinga, L. M. K. Vandersypen, and A. F. Morpurgo, *Nature (London)* **446**, 56 (2007).
⁹V. V. Cheianov, V. Fal'ko, and B. L. Altshuler, *Science* **315**, 1252 (2007).
¹⁰E. V. Castro, K. S. Novoselov, S. V. Morozov, N. M. R. Peres, J. M. B. Lopes dos Santos, J. Nilsson, F. Guinea, A. K. Geim, and A. H. Castro Neto, arXiv:cond-mat/0611342 (unpublished).
¹¹T. Ohta, A. Bostwick, T. Seyller, K. Horn, and E. Rotenberg,

- Science **313**, 951 (2006).
- ¹²G. Csanyi, P. B. Littlewood, A. H. Nevidomskyy, C. J. Pickard, and B. D. Simons, *Nat. Phys.* **1**, 42 (2006).
- ¹³B. Uchoa and A. H. Castro Neto, *Phys. Rev. Lett.* **98**, 146801 (2007).
- ¹⁴See, for instance, S. B. Fagan, R. Mota, A. J. R. da Silva, and A. Fazzio, *Phys. Rev. B* **67**, 205414 (2003), and references therein.
- ¹⁵M. Caragiu and S. Finberg, *J. Phys.: Condens. Matter* **17**, R995 (2005).
- ¹⁶S. B. Fagan, R. Mota, A. J. R. da Silva, and A. Fazzio, *J. Phys.: Condens. Matter* **16**, 3647 (2004); *Nanotechnology* **17**, 1 (2006).
- ¹⁷P. Blaha, K. Schwarz, G. K. H. Madsen, D. Kvasnicka, and J. Luitz, in *WIEN2k, An Augmented Plane Wave Local Orbitals Program for Calculating Crystal Properties*, edited by K. Schwarz (TU, Wien, Austria, 2001).
- ¹⁸J. P. Perdew, K. Burke, and M. Ernzerhof, *Phys. Rev. Lett.* **77**, 3865 (1996).
- ¹⁹V. I. Anisimov, I. V. Solovyev, M. A. Korotin, M. T. Czyzyk, and G. A. Sawatzky, *Phys. Rev. B* **48**, 16929 (1993).
- ²⁰A. I. Liechtenstein, V. I. Anisimov, and J. Zaanen, *Phys. Rev. B* **52**, R5467 (1995).
- ²¹D. Lamoien and B. N. J. Persson, *J. Chem. Phys.* **108**, 3332 (1998).
- ²²F. Ancilotto and F. Toigo, *Phys. Rev. B* **47**, 13713 (1993).
- ²³Z. Y. Li, K. M. Hock, and R. E. Palmer, *Phys. Rev. Lett.* **67**, 1562 (1991).
- ²⁴M. Posternak, A. Baldereschi, A. J. Freeman, E. Wimmer, and M. Weinert, *Phys. Rev. Lett.* **50**, 761 (1983).
- ²⁵Y. Miyamoto, A. Rubio, X. Blase, M. L. Cohen, and S. G. Louie, *Phys. Rev. Lett.* **74**, 2993 (1995).
- ²⁶E. R. Margine and V. H. Crespi, *Phys. Rev. Lett.* **96**, 196803 (2006).
- ²⁷K. Rytkonen, J. Akola, and M. Manninen, *Phys. Rev. B* **75**, 075401 (2007).
- ²⁸On top of a stack of graphite layers, the alkaline adatoms induce the opening of a gap of ~ 0.15 eV in the surface states of graphite due to the symmetry of the Bernal staking. See M. Pivetta, F. Patthey, I. Barke, H. Hovel, B. Delley, and W.-D. Schneider, *Phys. Rev. B* **71**, 165430 (2005).
- ²⁹L. Lou, L. Sterlund, and B. Hellsing, *J. Chem. Phys.* **112**, 4788 (2000).
- ³⁰O. Gunnarsson, *Rev. Mod. Phys.* **69**, 575 (1997).
- ³¹J. M. McChesney, A. Bostwick, T. Ohta, K. V. Emtsev, T. Seyller, K. Horn, and E. Rotenberg, arXiv:0705.3264 (unpublished).
- ³²J. Algdal, M. Breitholtz, T. Kihlgren, S. A. Lindgren, and L. Wallden, *Phys. Rev. B* **73**, 165409 (2006).
- ³³D. P. DiVincenzo and S. Rabii, *Phys. Rev. B* **25**, 4110 (1982).
- ³⁴C. Hartwigsen, W. Witschel, and E. Spohr, *Phys. Rev. B* **55**, 4953 (1997).
- ³⁵R. Pfandzelter, G. Steierl, and C. Rau, *Phys. Rev. Lett.* **74**, 3467 (1995).
- ³⁶A. Goldoni, A. Baraldi, G. Comelli, S. Lizzit, and G. Paolucci, *Phys. Rev. Lett.* **82**, 3156 (1999).
- ³⁷B. Sampedro, P. Crespo, A. Hernando, R. Litrán, J. C. Sánchez López, C. López Cartes, A. Fernandez, J. Ramírez, J. González Calbet, and M. Vallet, *Phys. Rev. Lett.* **91**, 237203 (2003).
- ³⁸H. Chen, N. E. Brener, and J. Callaway, *Phys. Rev. B* **40**, 1443 (1989).
- ³⁹W. F. Egelhoff and G. G. Tibbetts, *Phys. Rev. B* **19**, 5028 (1979).
- ⁴⁰A. Goldoni, A. Baraldi, G. Comelli, F. Esch, R. Larciprete, S. Lizzit, and G. Paolucci, *Phys. Rev. B* **63**, 035405 (2000).
- ⁴¹T. Nautiyal, T. H. Rho, and K. S. Kim, *Phys. Rev. B* **69**, 193404 (2004).
- ⁴²L. Chen, L. Chen, R. Wu, N. Kioussis, and J. R. Blanco, *J. Appl. Phys.* **81**, 4161 (1997).
- ⁴³F. Valencia, A. H. Romero, F. Ancilotto, and P. L. Silvestrelli, *J. Phys. Chem. B* **110**, 14832 (2006).